Limnology (2009) 10:135–141
DOI 10.1007/s10201-009-0263-y

NOTE

Remote-sensing assessment of regional inland lake water clarity in northeast China

Hongtao Duan · Ronghua Ma · Yuanzhi Zhang · Bai Zhang

Received: 27 August 2008 / Accepted: 12 February 2009 / Published online: 12 March 2009

Abstract Water clarity in three lakes, Chagan, Xinmiao, and Kuli, in northeast China was evaluated based on Landsat TM data and in situ measurements in this study. The agreement between satellite data and water clarity from field-collected Secchi disk depth (SDD) for individual lakes was strong ($0.72 \leq R^2 \leq 0.98$), and four regression equations were used to estimate SDD values. Lake clarity showed strong geographic patterns: Lake Chagan had low clarity and Lake Xinmiao and Kuli had high clarity. The study indicates that Landsat TM can be effectively applied to estimate water clarity for inland lakes in the area.

Keywords Secchi disk depth · Lake Chagan · Satellite data

Introduction

Lakes are valuable water resources and used for fishing, transportation, agriculture, industry, recreation, and tourism (Giardino et al. 2001). Water-quality conditions for numerous lakes around the world are so badly deteriorated that eutrophication is one of the most severe environmental problems (Khan and Ansari 2005). Protecting and monitoring lake water quality is a major concern for many federal and local agencies and citizen groups (Olmanson et al. 2008). Water clarity, usually measured with a Secchi disk, is a good indicator of user perception of water quality in lakes (Heiskary and Walker 1988), and the wide range of water clarity likely reflects both natural characteristics (e.g., depth, area, and watershed) and effects of anthropogenic characteristics (i.e., land-use and management practices) (Olmanson et al. 2008). Therefore, it is essential to find an easy and fast way to monitor and assess water quality in inland lakes.

Remote sensing from space-based platforms can provide meaningful information for enhancing regional monitoring and assessment of lake water quality and trophic conditions. Lathrop and Lillesand (1986) used the Landsat Thematic Mapper (TM) green band to estimate Secchi disk depth (SDD) in Green Bay and central Lake Michigan. Giardino et al. (2001) used the blue/green ratio (TM1/TM2) to estimate the euphotic-zone depth in Lake Iseo, Italy. Olmanson et al. (2008) assembled a 20-year comprehensive water clarity database from Landsat TM and ETM+ for Minnesota lakes larger than 8 ha in surface area; it contains data on more than 10,500 lakes at 5-year intervals over the period 1985–2005. Satellite images have been widely used to monitor water quality (Dekker and Peters 1993; Schneider and Mauser 1996; Zilioli and Brivio 1997; Fraser 1998a, b; Giardino et al. 2001; Wu et al. 2008), and the Landsat system is particularly useful for assessment of inland lakes due to the combination of temporal coverage, spatial resolution, and data availability (Kloiber et al. 2002).

The general approach used in previous applications of Landsat imagery for estimating lake clarity has been regression analysis of Landsat broad-band reflectance and

H. Duan (✉) · R. Ma
State Key Laboratory of Lake Science and Environment,
Nanjing Institute of Geography and Limnology,
Chinese Academy of Sciences, 210008 Nanjing, China
e-mail: htduan@niglas.ac.cn

Y. Zhang
Institute of Space and Earth Information Science,
The Chinese University of Hong Kong,
Shatin, NT, Hong Kong

B. Zhang
Northeast Institute of Geography and Agricultural Ecology,
Chinese Academy of Sciences, 130012 Changchun, China

nearly contemporaneous ground observation data (Kloiber et al. 2002). However, these results lack consistency, do not show causal relationships clearly, and rely on frequent water-quality sampling during satellite passages (Lindell et al. 1999). Analytical algorithms based on radiative transfer theory are expected to be accurately applied to a variety of regions; however, they require absorption and backscattering coefficients, which also differ in different research areas. Advanced studies are being carried out by a few experienced authors and are difficult for routine application. Therefore, we have to trust the simple regression correlation techniques used previously, which are very simple to use and sometimes give results as good as analytical models (Giardino et al. 2001).

The overall objective of this study is to develop a method for using remote sensing to estimate water clarity for lake management in northeast China. Intensive field data collected concurrently with satellite overpasses were used to empirically derive a model to estimate SDD from Landsat-5 TM data.

Materials and methods

Study area

The study area of three lakes is located in the Jilin Province of northeast China. Lake Chagan, Lake Xinmiao, and Lake Kuli cover about 416 km^2 (see Fig. 1). Lake Kuli is isolated from the other two lakes, while Lake Chagan and Lake Xinmiao are connected to each other by a canal. Since the Songhua River first flows into Lake Xinmiao through a canal and then runs out of Lake Chagan, the Songhua River is the main source feeding the lakes region (Duan et al. 2008).

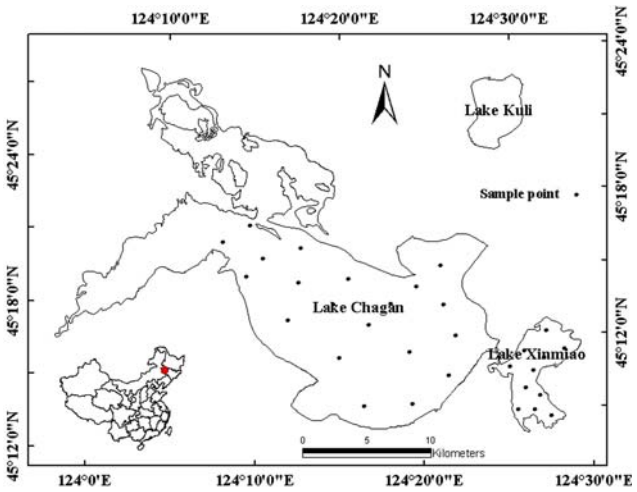

Fig. 1 Location of the Chagan Lake District in China

Water-sampling and satellite-image data

Water sampling and measurements were performed on 26 July 2004, 14 October 2004, and 13 July 2005 (Table 1). Water sampling and fieldwork were conducted in Lake Chagan and Lake Xinmiao, but not Lake Kuli. However, we collected some data for Lake Kuli in July 2005 from the local monitoring stations to compare with our estimated results. In each fieldwork episode, the position of the sampling boat was geo-located by a portable Ashtech ProMark2 Global Positioning System (GPS) receiver with 0.3- to 3-m accuracy specification. SDD was measured at the selected points of the lakes with a 20-cm-diameter disk painted in black/white quarters (Chen et al. 2007).

Three cloud-free Landsat TM images were selected for data analysis on the same days as our fieldwork. On each of these three days, weather conditions were adequate with a windspeed below 5 m s^{-1} and no cloud cover in the study area. For the TM data geo-coding, one TM image was first geometrically corrected using ground control points (GCPs) with ENVI software. Ten GCPs were acquired by the GPS receiver to rectify the TM image of the three lakes. The TM image was also resampled using the nearest-neighbor method to preserve its radiometry. The other two TM images were geo-coded to that TM scene as their master image. Atmospheric correction was performed using the 6S (Second Simulation of Satellite Signal in the Solar Spectrum) model (Lee and Kaufman 1986; Ghulam et al. 2004). This model corrects at-sensor radiance images for solar illuminance, and Rayleigh and aerosol scattering. The input to the 6S specifies geometrical, spectral, and atmospheric and target conditions, which were obtained from local weather stations. More details can be seen in our previous paper (Duan et al. 2008).

Table 1 Sample number and Secchi disk depth in Lake Chagan and Lake Xinmiao

	26 July 2004	14 October 2004	13 July 2005
Lake Chagan			
Number	8	20	19
Min (cm)	22	10	19
Max (cm)	24	27	37
Mean (cm)	23	14	26
Lake Xinmiao			
Number	7	11	–
Min (cm)	23	38	–
Max (cm)	79	55	
Mean (cm)	46	47	

Results and discussion

Empirical regression models

Previous investigations (Lathrop 1992; Lavery et al. 1993; Kloiber et al. 2002) have suggested that band combinations such as ratios, multiplication, and averages provided useful relationships, and all were carried out using the averaged pixel digital numbers (DNs). In this study, a 3 × 3 pixel window corresponding to an area of 90 × 90 m was extracted from the images after atmospheric correction of each water-sampling test site. Water clarity (SDD) retrievals were examined empirically by deriving the regression algorithms for all possible band combinations and selecting the one with the highest correlation coefficient (R) or coefficient of determination (R^2). These parameters are given in Tables 2, 3, and 4. TM bands or their combinations were employed to estimate SDD as follows:

$$Y = AX + B \quad (1)$$

where Y is SDD (cm) and X refers to the reflectance of a single TM band or a combination.

Logarithmic transformation of variables was suggested to determine the goodness of fit for SDD models (Harma et al. 2001; Kloiber et al. 2002). This method complicates the comparison of different models by means of the determination of coefficients, but the R^2 results in a slight improvement of 5–6% higher than those of above. This approach has been proven to be successful in regression equations used to estimate SDD. Table 5 shows that logarithmic transformation increased the R^2 values, except in October 2004. The equation is always shown as follows:

$$\ln(Y) = A \ln(X) + B \quad (2)$$

where Y is SDD (cm) and X refers to the reflectance of a single TM band or their combinations.

Applying Eqs. 1–2, Fig. 2a shows a good regression between TM data and in situ SDD, with $R^2 = 0.9074$ for the two lakes (Chagan and Xinmiao) in July 2004. Since SDD was high for TM data in Lake Xinmiao in July 2004 with $R^2 = 0.9843$ (Fig. 2b), the regression equation from Fig. 2a was only used to derive SDD in Lake Chagan in July 2004, and the equation from Fig. 2b was applied in Lake Xinmiao in July 2004. We also found that SDD for the two lakes was best estimated from TM data in October 2004, with $R^2 = 0.9447$ (Fig. 2c). Figure 2d in Lake Chagan from Eq. 2 indicates that TM data in July 2005 can be used to retrieve SDD with $R^2 = 0.7241$ for the three lakes, since there were no in situ data for the other two lakes in July 2005. The models developed for different seasons were applied to Landsat data for the sample of pixels from each lake to calculate water clarity (SDD) and showed good estimation accuracy with low RMSE (Fig. 2a–d).

Suspended matter and phytoplankton pigment cause reflectance peaks in the wavelength of Landsat TM bands (Lathrop and Lillesand 1986; Dekker and Peters 1993). Longer wavelengths are absorbed by clear water; therefore, suspended particles and chlorophyll will increase the amount of spectral energy returned to the sensor for aquatic

Table 2 Individual or combined TM bands 1–4 and their relation to SDD presented as correlation coefficient (R). Data from 26 July 2004 for Lakes Chagan and Xinmaio

Variables	R (both lakes)	R (Chagan)	R (Xinmiao)	Variables	R (both lakes)	R (Chagan)	R (Xinmiao)
TM1	−0.8240	−0.3514	−0.8868	A.V. (1, 2, 3)	−0.8561	−0.6058	−0.9174
TM2	−0.8481	−0.2755	−0.9289	A.V. (1, 2, 4)	−0.8428	−0.2306	−0.9103
TM3	−0.8804	−0.6219	−0.9252	A.V. (2, 3, 4)	−0.8628	−0.4954	−0.9218
TM4	−0.8498	0.1654	−0.8534	A.V. (1, 3, 4)	−0.8600	−0.5781	−0.9116
TM4/TM1	−0.6521	0.3625	−0.5773	A.V. (1, 2, 3, 4)	−0.8576	−0.5236	−0.9167
TM4/TM2	0.8301	0.3446	0.7258	TM1 × TM2	−0.7898	−0.3314	−0.8939
TM4/TM3	−0.1166	0.5420	0.1553	TM1 × TM3	−0.8176	−0.6693	−0.8945
TM3/TM2	0.9350	−0.3466	0.8800	TM1 × TM4	−0.8045	−0.0875	−0.8542
TM3/TM1	−0.7427	−0.3035	−0.9789	TM2 × TM3	−0.8021	−0.5501	−0.8827
TM2/TM1	−0.9337	0.0350	−0.9557	TM2 × TM4	−0.7947	−0.0685	−0.8554
A.V. (3, 4)	−0.8754	−0.4989	−0.9153	TM3 × TM4	−0.8267	−0.3548	−0.8588
A.V. (2, 4)	−0.8528	−0.0630	−0.9120	TM1 × TM1	−0.7874	−0.3607	−0.8776
A.V. (1, 4)	−0.8391	−0.1914	−0.8952	TM2 × TM2	−0.7665	−0.2845	−0.8484
A.V. (3, 2)	−0.8694	−0.6046	−0.9274	TM3 × TM3	−0.8311	−0.6189	−0.8959
A.V. (3, 1)	−0.8586	−0.6843	−0.9119	TM4 × TM4	−0.8056	0.1599	−0.8078
A.V. (2, 1)	−0.8357	−0.3353	−0.9100				

A.V. Average

Table 3 Individual or combined TM bands 1–4 and their relation to SDD presented as correlation coefficient (*R*). Data from 14 October 2004 for Lakes Chagan and Xinmaio

Variables	*R* (both lakes)	*R* (Chagan)	*R* (Xinmiao)	Variables	*R* (both lakes)	*R* (Chagan)	*R* (Xinmiao)
TM1	−0.9608	−0.4726	−0.0103	A.V. (1, 2, 3)	−0.9647	−0.4629	−0.5196
TM2	−0.9618	−0.4597	−0.0958	A.V. (1, 2, 4)	−0.9707	−0.5280	−0.8894
TM3	−0.9637	−0.3256	−0.7922	A.V. (2, 3, 4)	−0.9704	−0.4667	−0.8857
TM4	−0.9706	−0.4866	−0.8590	A.V. (1, 3, 4)	−0.9710	−0.5005	−0.8869
TM4/TM1	−0.9487	−0.2798	−0.8497	A.V. (1, 2, 3, 4)	−0.9699	−0.4995	−0.8901
TM4/TM2	0.3643	−0.2104	−0.8556	TM1 × TM2	−0.9653	−0.4939	−0.0621
TM4/TM3	−0.9476	−0.4632	−0.8391	TM1 × TM3	−0.9672	−0.4544	−0.5612
TM3/TM2	0.4103	0.4650	−0.6498	TM1 × TM4	−0.9640	−0.5318	−0.8690
TM3/TM1	−0.7291	0.3420	−0.8491	TM2 × TM3	−0.9659	−0.4328	−0.0711
TM2/TM1	−0.9157	−0.1816	−0.1353	TM2 × TM4	−0.9550	−0.4976	−0.2906
A.V. (3, 4)	−0.9718	−0.4578	−0.8774	TM3 × TM4	−0.9644	−0.4729	−0.8670
A.V. (2, 4)	−0.9714	−0.4976	−0.8755	TM1 × TM1	−0.9587	−0.4671	−0.0006
A.V. (1, 4)	−0.9720	−0.5324	−0.8792	TM2 × TM2	−0.9592	−0.4627	0.1620
A.V. (3, 2)	−0.9638	−0.3954	−0.6738	TM3 × TM3	−0.9663	−0.3314	−0.8256
A.V. (3, 1)	−0.9650	−0.4495	−0.6130	TM4 × TM4	−0.9422	−0.4887	−0.8563
A.V. (2, 1)	−0.9631	−0.4978	−0.0471				

A.V. Average

Table 4 Individual or combined TM bands 1–4 and their relation to SDD presented as correlation coefficient (*R*). Data from 13 July 2005

Variables	*R*	Variables	*R*
TM1	−0.7258	A.V. (1, 2, 3)	−0.8119
TM2	−0.8035	A.V. (1, 2, 4)	−0.7833
TM3	−0.8149	A.V. (2, 3, 4)	−0.7774
TM4	−0.4635	A.V. (1, 3, 4)	−0.8122
TM4/TM1	−0.2059	A.V. (1, 2, 3, 4)	−0.8212
TM4/TM2	−0.0031	TM1 × TM2	−0.8077
TM4/TM3	0.0544	TM1 × TM3	−0.7927
TM3/TM2	−0.2022	TM1 × TM4	−0.6425
TM3/TM1	−0.7574	TM2 × TM3	−0.8234
TM2/TM1	−0.5573	TM2 × TM4	−0.6384
A.V. (3, 4)	−0.7384	TM3 × TM4	−0.6931
A.V. (2, 4)	−0.6403	TM1 × TM1	−0.7207
A.V. (1, 4)	−0.7442	TM2 × TM2	−0.8007
A.V. (3, 2)	−0.8293	TM3 × TM3	−0.8064
A.V. (3, 1)	−0.7898	TM4 × TM4	−0.4288
A.V. (2, 1)	−0.7949		

A.V. Average

feature detection (Lathrop 1992). Since SDD is poorly correlated with chlorophyll *a* ($R = -0.33$) in these lakes, suspended particles will determine the water transparency, as previous research has revealed (Yu et al. 1993). Therefore, TM bands that measure suspended solids would likely be inversely related to SDD (Allee and Johnson 1999). TM 3 and TM 4 bands in red and infrared wavelengths always have a high sensitivity to suspended matter (Lavery et al. 1993; Zilioli and Brivio 1997; Giardino et al. 2001). In Tables 2, 3, and 4, correlation results from many TM band combinations are listed, and TM 3 and/or TM 4 with their band combinations were well correlated with SDD in this study. However, due to the changing water quality in different lakes and seasons, there is a lack of consistency in which TM bands are expected to be best related to SDD. The regression line (Eq. 1 and 2) of the best band combination changes day-by-day (Table 5). Therefore, these results do not show causal relationships clearly and would require on frequent water-quality sampling during satellite passages. In the meantime, we have to trust the more simple regression correlation techniques, which are very easy to use and sometimes give results as good as analytical models (Giardino et al. 2001).

Evaluation of water clarity from Landsat data

Lake Chagan always presented a lower SDD level between 0.09 and 0.46 m throughout 2004 (Table 1). In contrast, Lake Xinmiao had a higher SDD level between 0.23 and 0.96 m in 2004 (Table 1). This is because the water supply from Songhua River through a canal first flows into Lake Xinmiao from its southern corner, and then runs into Lake Chagan and finally out of Lake Chagan. In addition, the south area of Lake Xinmaio is crowded with aquatic plants. Therefore, Lake Xinmiao has good water quality and higher SDD. However, due to its larger area and shallow depth with a loose mud bed that easily floats off on windy days, Lake Chagan has a poor transparency. Generally,

Table 5 Regression model between SDD and Landsat TM data for Lake Xinmaio and Lake Chagan

Date	Lakes	Band combination	Regression model	R^2
26-07-2004	Both lakes	TM3/TM2	$y = 11.126x + 1.5642$	0.87
			$\ln(y) = 0.9779\ln(x) + 2.4729$	0.91
	Lake Xinmiao	TM3/TM1	$y = -195.28x + 235.48$	0.96
			$\ln(y) = -4.0655\ln(x) + 3.6085$	0.98
14-10-2004	Both lakes	A.V. (1, 4)	$y = -415.43x + 64.293$	0.94
			$\ln(y) = -1.1588\ln(x) + 0.1782$	0.92
13-07-2005	Lake Chagan	A.V. (3, 2)	$y = -572.55x + 77.579$	0.69
			$\ln(y) = -1.9373\ln(x) - 1.4269$	0.72

x refers to the reflectance of TM band combinations, y represents SDD

A.V. average

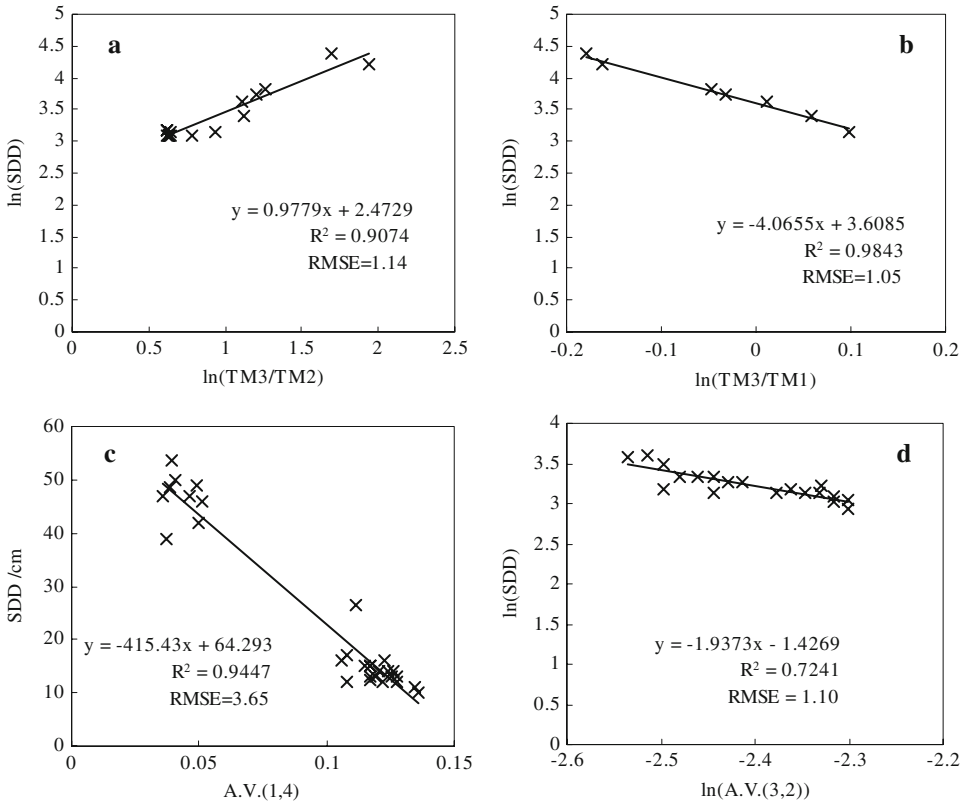

Fig. 2 Regression relationships between Secchi disk depth and TM data. **a** Two lakes (Chagan and Xinmiao) on 26 July 2004. **b** Lake Xinmiao on 26 July 2004. **c** Two lakes (Chagan and Xinmiao) on 14 October 2004. **d** Lake Chagan on 13 July 2005

during the same season in different years, Lake Chagan has a lower SDD level, Lake Xinmiao a higher level, and Lake Kuli falls between the two. Figure 3a shows that the SDD level ranged from 20 to 26 cm in Lake Chagan in July 2004. Since the water of Lake Xinmiao runs into Lake Chagan through an inlet from the south, the SDD level in the southern entrance of Lake Chagan was between 23 and 26 cm. The SDD level in Lake Xinmiao, however, decreased gradually from the south at 60–90 cm to its northern bank up to the level of 20–23 cm. Lake Kuli, as an isolated lake, had an SDD level of 26–30 cm in general.

From Fig. 3c, we found that, in general, the SDD levels of the three lakes in July 2005 were clearly higher than those of the three lakes in July 2004 (Fig. 3a), except for the southern part of Lake Xinmiao. In July 2005, SDD levels in Lake Chagan were classified into four classes: a smaller area near its southern entrance had an SDD level of 40–45 cm, the central part had an SDD level of 35–40 cm, some outer central areas 23–30 cm, and the small northern edge areas 10–23 cm. Lake Xinmiao was divided into three classes from its south to its north: 55–60, 50–55, and 40–50 cm. Lake Kuli was also divided into two classes from

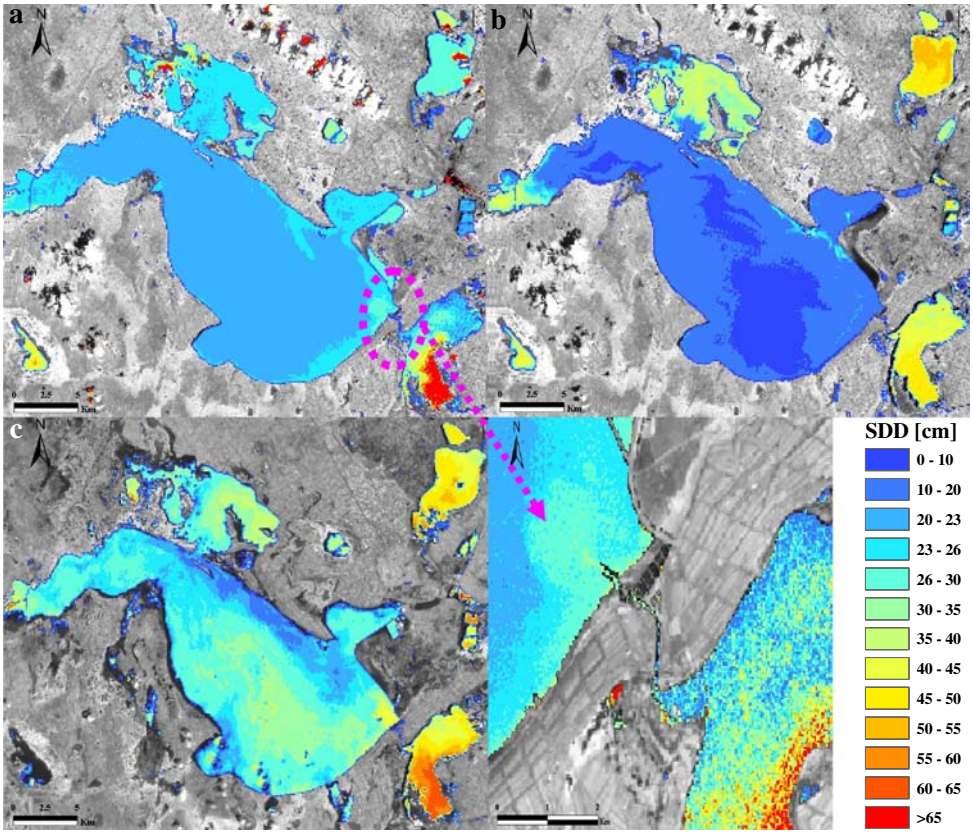

Fig. 3 SDD levels estimated from the TM data. **a** 26 July 2004. **b** 14 October 2004. **c** 13 July 2005

the inside to the outside: 50–55 and 45–50 cm. In addition, it is obvious that SDD levels in Lake Chagan were lower in October 2004 (Fig. 3b) than those in July 2004 (Fig. 3a). We observed the lowest SDD level at 0–10 cm was distributed in the central part of Lake Chagan. In contrast, the majority of Lakes Xinmiao and Kuli had a higher SDD level (40–55 cm) in October 2004 than in July 2004.

By comparing the SDD levels of the three lakes in July with those in October for both 2004 and 2005, we found that the SDD level in the summer was much higher than in the late autumn during the yearly cycle. The main reasons are probably that there are more windy days to stir up loose mud beds in this season. Additionally, when comparing one season (e.g., in the summer) across different years, we noted that the general SDD level in July 2004 was lower than that in July 2005. This is because of the fact that the summer of 2005 had more rainfall and more water supply than the summer of 2004 over the lakes' region.

Acknowledgments We would like to thank the Special Prize of President Scholarship for Postgraduate Students of the Chinese Academy of Sciences (No. 07YJ011001), the Knowledge Innovation Program of the Chinese Academy of Sciences (No. CXNI-GLAS200807), and the National Natural Science Foundation of China (No. 40801137, 40871168) for providing financial support. Thanks are also due to two anonymous reviewers who offered helpful suggestions.

References

Allee RJ, Johnson JE (1999) Use of satellite imagery to estimate surface chlorophyll a and Secchi disc depth of Bull Shoals Reservoir, Arkansas, USA. Int J Remote Sens 20:1057–1072. doi:10.1080/014311699212830

Chen Z, Muller-Karger FE, Hu C (2007) Remote sensing of water clarity in Tampa Bay. Remote Sens Environ 109:249–259. doi:10.1016/j.rse.2007.01.002

Dekker AG, Peters SWM (1993) The use of the Thematic Mapper for the analysis of eutrophic lakes: a case study in the Netherlands. Int J Remote Sens 14:799–821. doi:10.1080/01431169308904379

Duan H, Zhang Y, Zhang B, Song K, Wang Z, Liu D, Li F (2008) Estimation of chlorophyll-a concentration and trophic states for inland lakes in Northeast China from Landsat TM data and field spectral measurements. Int J Remote Sens 29:767–786. doi:10.1080/01431160701355249

Fraser RN (1998a) Hyperspectral remote sensing of turbidity and chlorophyll a among Nebraska Sand Hills lakes. Int J Remote Sens 19:1579–1589. doi:10.1080/014311698215360

Fraser RN (1998b) Multispectral remote sensing of turbidity among Nebraska Sand Hills lakes. Int J Remote Sens 19:3011–3016. doi:10.1080/014311698214406

Ghulam A, Qin Q, Zhu L, Abdrahman P (2004) Satellite remote sensing of groundwater: quantitative modelling and uncertainty reduction using 6S atmospheric simulations. Int J Remote Sens 25:5509–5524. doi:10.1080/01431160410001719821

Giardino C, Pepe M, Brivio PA, Ghezzi P, Zilioli E (2001) Detecting chlorophyll, Secchi disk depth and surface temperature in a sub-alpine lake using Landsat imagery. Sci Total Environ 268:19–29. doi:10.1016/S0048-9697(00)00692-6

Harma P, Vepsalainen J, Hannonen T, Pyhalahti T, Kamari J, Kallio K, Eloheimo K, Koponen S (2001) Detection of water quality using simulated satellite data and semi-empirical algorithms in Finland. Sci Total Environ 268:107–121. doi:10.1016/S0048-9697(00)00688-4

Heiskary SA, Walker WWJr (1988) Developing phosphorus criteria for Minnesota lakes. Lake Reservoir Manage 4:1–9

Khan FA, Ansari AA (2005) Eutrophication: an ecological vision. Bot Rev 71:449–482. doi:10.1663/0006-8101(2005)071

Kloiber SM, Brezonik PL, Olmanson LG, Bauer ME (2002) A procedure for regional lake water clarity assessment using Landsat multispectral data. Remote Sens Environ 82:38–47. doi:10.1016/S0034-4257(02)00022-6

Lathrop RG (1992) Landsat Thematic Mapper monitoring of turbid inland water quality. Photogramm Eng Remote Sens 58:465–470

Lathrop RG, Lillesand TM (1986) Use of Thematic Mapper data to assess water quality in Green Bay and Central Lake Michigan. Photogramm Eng Remote Sens 52:671–680

Lavery P, Pattiaratchi C, Wyllie A, Hick P (1993) Water quality monitoring in estuarine waters using the Landsat Thematic Mapper. Remote Sens Environ 46:268–280. doi:10.1016/0034-4257(93)90047-2

Lee T, Kaufman Y (1986) Non-Lambertian effects on remote-sensing of surface reflectance and vegetation index. IEEE Trans Geosci Remote Sens 24:699–708. doi:10.1109/TGRS.1986.289617

Lindell T, Pierson D, Premazzi G, Zilioli E (1999) Manual for monitoring European lakes using remote sensing techniques. Report EUR 18665. Office for Official Publications of the European Communities, Luxembourg

Olmanson LG, Bauer ME, Brezonik PL (2008) A 20-year Landsat water clarity census of Minnesota's 10,000 lakes. Remote Sens Environ 112(11):4086–4097. doi:10.1016/j.rse.2007.12.013

Schneider K, Mauser W (1996) Processing and accuracy of Landsat thematic mapper for lake surface temperature measurement. Int J Remote Sens 11:2027–2041. doi:10.1080/01431169608948757

Wu GF, Leeuw JD, Skidmore AK, Prins HHT, Liu Y (2008) Comparison of MODIS and Landsat TM5 images for mapping tempo-spatial dynamics of Secchi disk depths in Poyang Lake National Nature Reserve, China. Int J Remote Sens 29:2183–2198. doi:10.1080/01431160701422254

Yu MR, Shen SD, Zhu MY (1993) The eco-environment changes and the use of protection in Lake Chagan (in Chinese). Jilin Water Resour 5:22–24

Zilioli E, Brivio PA (1997) The satellite derived optical information for the comparative assessment of lacustrine water quality. Sci Total Environ 196:229–245. doi:10.1016/S0048-9697(96)05411-3